Mol. Cells *27*, 481-490, April 30, 2009
DOI/10.1007/s10059-009-0054-7

Molecules and Cells

©2009 KSMCB

Temporal and Spatial Expression Patterns of Nine *Arabidopsis* Genes Encoding Jumonji C-Domain Proteins

Eun-Hye Hong[1,2,5], Young-Min Jeong[1,2,3,5], Jee-Youn Ryu[1,2], Richard M. Amasino[2,3], Bosl Noh[2,4,*], and Yoo-Sun Noh[1,2,*]

Diverse posttranslational modifications of histones, such as acetylation and methylation, play important roles in controlling gene expression. Histone methylation in particular is involved in a broad range of biological processes, including heterochromatin formation, X-chromosome inactivation, genomic imprinting, and transcriptional regulation. Recently, it has been demonstrated that proteins containing the Jumonji (Jmj) C domain can demethylate histones. In *Arabidopsis*, twenty-one genes encode JmjC domain-containing proteins, which can be clustered into five clades. To address the biological roles of the *Arabidopsis* genes encoding JmjC-domain proteins, we analyzed the temporal and spatial expression patterns of nine genes. RT-PCR analyses indicate all nine *Arabidopsis thaliana Jmj* (*AtJmj*) genes studied are actively expressed in various tissues. Furthermore, studies of transgenic plants harboring *AtJmj::β-glucuronidase* fusion constructs reveal that these nine *AtJmj* genes are expressed in a developmentally and spatially regulated manner.

INTRODUCTION

In eukaryotic cells, nuclear DNA is part of a complex structure called chromatin, which is composed of nucleosomes in which DNA wraps around the histone proteins. Histones, in particular their N-terminal tails, are often posttranslationally subjected to covalent modifications, such as acetylation, methylation, phosphorylation, sumoylation, ubiquitylation, deimination, and ribosylation (Kouzarides, 2007). Among these various modifications, histone methylation is recognized as an important epigenetic marker in regulating a wide range of biological processes, such as heterochromatin formation, X-chromosome inactivation, genomic imprinting, transcriptional regulation, and DNA repair (reviewed in Kouzarides, 2007; Kwon and Workman, 2008). Histone methylation occurs on specific residues such as lysine and arginine of histone H3 and H4; lysine residues of histones can be mono-, di-, or trimethylated by lysine histone methyltransferase. In contrast, arginine residues can be monomethylated or asymmetrically/symmetrically dimethylated by arginine methyltransferases (PRMTs; Zhou and Ma, 2008). The effects of such methylations on the transcription and the chromatin structure differ, depending on the positions of modifications. For example, methylations at histone H3 lysine 9 (H3K9), H3K27, and H4K20 are generally associated with heterochromatin formation and gene silencing, resulting in the suppression of gene expression. In contrast, methylations at H3K4, H3K36 and H3K79 are involved in the activation of transcription (Martin and Zhang, 2005).

Histone methylation has long been thought to be an irreversible epigenetic modification (Byvoet, 1972; Duerre and Lee, 1974); however, the recent discovery of histone demethylases indicates that histone methylation is a reversible and dynamically regulated process. Three classes of enzymes are currently known to have histone demethylation activity. First, the histone deiminase, Peptidylarginine Deiminase 4 (PADI4), was reported to be able to remove methyl groups from arginine residues by converting methylated H3 arginine to citrulline. However, it is difficult to conclude that PADI4 has innate histone demethylase activity in vivo because it generates citrulline instead of an unmodified arginine (Cuthbert et al., 2004). A nuclear amine oxidase, Lysine-Specific Demethylase 1 (LSD1), was the first protein identified as an inherent histone demethylase. LSD1 specifically demethylates both mono- and dimethylated H3K4 via flavin adenine dinucleotide (FAD)-dependent oxidative reaction. Because LSD1 requires a protonated nitrogen for histone demethylation, it cannot remove methyl groups from tri-methylated histone (Shi et al., 2004). This suggests that there should be another histone demethylase that does not require protonated nitrogen. Shortly after the discovery of LSD1, a third family of histone demethylases was identified as having a conserved catalytic motif, the Jumonji (Jmj) C domain (Tsukada et al., 2006). Unlike LSD1, JmjC domain-containing proteins are capable of demethylating all of the mono-, di- and

[1]School of Biological Sciences, Seoul National University, Seoul 151-747, Korea, [2]Global Research Laboratory for Floral Regulatory Signaling, Seoul National University, Seoul 151-747, Korea, [3]Department of Biochemistry, University of Wisconsin, Madison, Wisconsin 53706, USA, [4]Environmental Biotechnology National Core Research Center, Gyeongsang National University, Jinju 660-701, Korea, [5]These authors contributed equally to this work.
*Correspondence: ysnoh@snu.ac.kr (YSN); bnoh2003@yahoo.co.kr (BN)

Received February 2, 2009; accepted February 10, 2009; published online April 13, 2009

Keywords: *Arabidopsis*, demethylase, epigenetics, histone demethylation, Jumonji

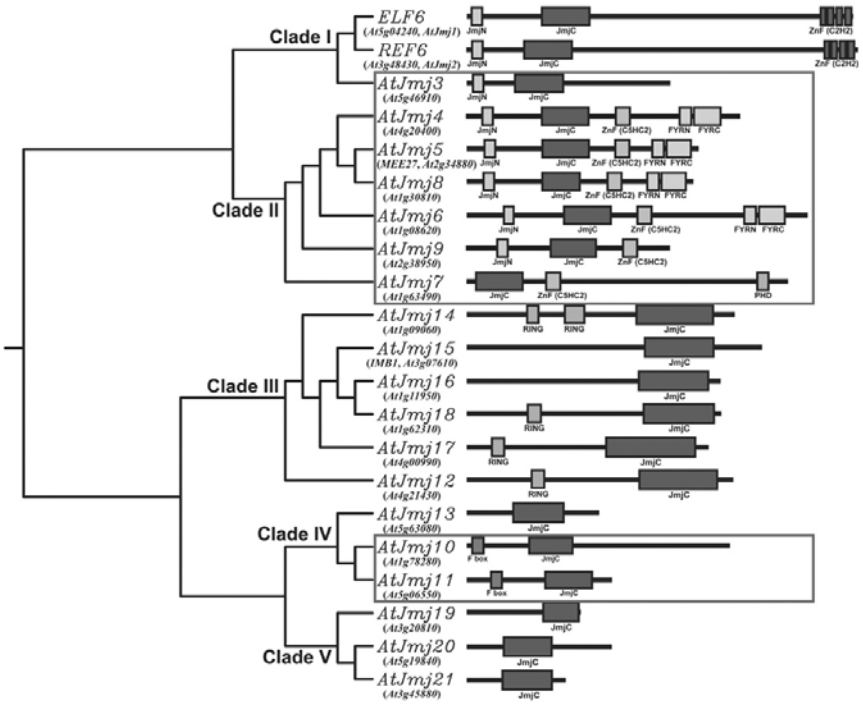

Fig. 1. Phylogenetic tree of twenty-one *Arabidopsis* JmjC domain-containing proteins. Tree was generated by ClustalW (Thompson et al., 1994; http://align.genome.jp/). Domains predict by SMART (http://smart.embl-heidelberg.de/) are indicated with domain names. AtJmj proteins analyzed in this study are in boxes.

trimethylated lysines of histones (Klose et al., 2006). In addition to lysines, they are also capable of removing methylation from arginines (Chang et al., 2007). JmjC domain-containing proteins exhibit specificity for histone residues or the state of methylation at specific residues: JHDM3/JMJD2A has a preference for H3K9 and H3K36 (Klose et al., 2006); JMJD2C demethylates di- and trimethylated H3K9 (Cloos et al., 2006); UTX and JMJD3 demethylates mono-, di-, and trimethylated H3K27 (Agger et al., 2007); and JARID1B removes methyl group from mono- , di- and trimethylated H3K4 (Xiang et al., 2007).

In plants, a large number of genes encoding JmjC domain-containing proteins have been identified in the genomes of *Arabidopsis*, rice, and poplar, mainly through bioinformatic approaches (Lu et al., 2008; Zhou and Ma, 2007). To date, only four of these genes encoding JmjC domain-containing proteins have been functionally characterized in *Arabidopsis*. The first characterized genes were *EARLY FLOWERING 6* (*ELF6*; *AtJmj1*) and *RELATIVE OF EARLY FLOWERING 6* (*REF6*; *AtJmj2*; see Fig. 1). Despite similarities in sequences and domain architectures, their biological functions are opposite each other: ELF6 acts as a floral repressor, whereas REF6 functions as a floral activator (Noh et al., 2004). REF6 is involved in histone modification at the central floral repressor, *FLOWERING LOCUS C* (*FLC*), locus. The third identified JmjC-domain protein, MEE27, is implicated in gametophyte development (Pagnussat et al., 2005), but its precise function is not yet clear. INCREASED EXPRESSION OF BONSAI METHYLATION 1 (IBM1), the fourth JmjC domain-containing protein, represses genic cytosine methylation, possibly through demethylation at H3K9 (Saze et al., 2008). Together, these reports indicate that JmjC domain-containing proteins play key roles in various aspects of development in plants, as they do in other organisms such as yeast and mammals. *Arabidopsis* has twenty-one genes encoding JmjC domain-containing proteins, including the four previously studied; thus, most remain uncharacterized. Therefore, in this study, as an initial approach to understand the roles of *Arabidopsis thaliana Jmj* (*AtJmj*) genes, we analyzed the phylogenetic relationship among them. We also examined the spatial and temporal expression patterns of nine *AtJmj* genes (from *AtJmj3* to *AtJmj11*).

MATERIALS AND METHODS

Plant materials and construction of *AtJmj::β-glucuronidase* (*GUS*) fusions

We used *Arabidopsis thaliana* ecotype Columbia. Plants were grown at 22°C either under long-day (16 h day/8 h night) or short-day (8 h day/16 h night) conditions. For the construction of *GUS* fusions, the promoter or genomic region of each *AtJmj* was amplified by polymerase chain reaction (PCR) using the primers listed in Table 1. The PCR products were then cloned into pPZP211-GUS (Noh and Amasino, 2003), and introduced into *Agrobacterium tumefaciens* strain ABI as described previously (Noh and Amasino, 2003).

Plant transformation and histochemical GUS assay

Agrobacterium strains carrying the *AtJmj::GUS* constructs were used to transform *Arabidopsis* plants by the floral dip method (Clough and Bent, 1998). Transgenic plants were selected on MS media containing 50 mg/L kanamycin. At least 20 independent transgenic plants for each *AtJmj::GUS* construct were screened on selective media and used for initial GUS assays to find a consistent expression pattern for each gene. Finally, a few representative transgenic lines for each construct were selected based on their consistent expression patterns and used to generate histochemical GUS-staining data. For histochemical GUS analysis, plants were fixed in 90% acetone solution on ice for 30 min and then washed twice with KPO_4 buffer. After fixation, plants were incubated in GUS-staining solution at 37°C for 15 min to overnight as described previously (Noh and Amasino, 2003). To clear tissues, 70% (v/v) ethanol was used (Jefferson et al., 1987). GUS expression patterns were analyzed using a stereo zoom microscope with HR for G6 conver-

Table 1. Oligonucleotides used for *GUS* fusion constructs

Gene	Product size (kb)	Name	Sequence
AtJmj3	3.6	JMJ3pr- F1	5′-gtcgacGGTCCATCTATTGGTCCCATTGAC-3′
(*At5g46910*)		JMJ3pr-Bam-R	5′-ATGggatccCATCAAGCCACCTCTCACAGTAGATG-3′
AtJmj4	1.6	JMJ4pr-Sal-F	5′-gtcgacGTCTCCTCTCTATCGCCATTCTTG-3′
(*At4g20400*)		JMJ4pr-Bam-R	5′-ggatccCATTTACAGTGAGATTAAGTTCAC-3′
AtJmj5	1.5	JMJ5-Sal-F	5′-gtcgacTTCAGC GACCTTCATCACCATTG-3′
(*At2g34880*)		JMJ5pr-Bam-R	5′-ggatccCATTGGATTGGAACCAATCACTC-3′
AtJmj6	2.3	JMJ6pr-Sal-F1	5′-gtcgacGAAGCCATTTCTCAGAATCCAGAAG-3′
(*At1g08620*)		JMJ6pr-Bam-R	5′-ggatccCATTACTTCTGTGCCAACACTAC-3′
AtJmj7	1.5	JMJ7-Sal-F1	5′-gtcgacACGTAGTACCTCTTCGATCATAAC-3′
(*At1g63490*)		JMJ7pr-Bam-R	5′-ggatccCATAACTTCAACCTCACCACCTG-3′
AtJmj8	1.7	JMJ8-Sal-F	5′-gtcgacTGCGAGTTCTTCTTTCAATGTG-3′
(*At1g30810*)		JMJ8pr-Bam-R	5′-ggatccCATATGAATTGAAAAATCAATAC-3′
AtJmj9	1.6	JMJ9-Sal-F1	5′-gtcgacGAACGGTCCCAATAGTTTAGGTG-3′
(*At2g38950*)		JMJ9pr-Bam-R	5′-ggatccCATTAAACCTTACAGCCACCAAAAG-3′
AtJmj10	5.6	JMJ10Fpr-Bam-F	5′-CATCggatccTGAGGATTCGTCGTGGTGAC-3′
(*At1g78280*)		JMJ10F-ORF-Bam-R	5′-CATggatccGTAGGTGTTAAGTAGACTCCAAACAG-3′
AtJmj11	3.0	JMJ11Fpr-Bam-F	5′-CAAAggatccTGTCCCAGAACGTAGATTG-3′
(*At5g06550*)		JMJ11F-ORF-Bam-R	5′-ATTGggatccGAAAGAAAACTTGAAAGTATC-3′

Restriction sites used for cloning are underlined

sion (with an LA-DC585 lens adapter) linked to a Canon PC 1086 or the Axio imager A1 with an Axiocam HRC (Carl Zeiss, Germany).

Reverse transcription (RT)-PCR

Total RNA was isolated by Tri-Reagent (Invitrogen, USA) from the following tissues: nine day (d)-old seedlings, roots from 9-d-old seedlings, leaves from 3-week-old plants, shoot apices plus young leaves, and flowers. In the case of flowers, tissues were collected from one-month-old plants. One microgram of total RNA was used for RT with Superscript II reverse transcriptase (Invitrogen, USA) following the instructions provided by the manufacturer. After completion of the RT reaction, 2 μl of first strand cDNA was amplified by PCR using the gene-specific primers listed in Table 2.

RESULTS

Phylogenetic analysis and domain comparison

In order to identify *Arabidopsis* genes encoding JmjC domain-containing proteins, we conducted BLAST searches of the *Arabidopsis* genomic DNA sequence database using the JmjC-domain sequences of ELF6 and REF6. We then compared the genes identified with this approach with the genes in the Chromatin Database (http://www.chromdb.org/). Finally, the twenty-one genes presumed to encode JmjC domain-containing proteins were designated *AtJmj1* to *AtJmj21* (Fig. 1).

Based on the sequence similarity between JmjC domains and characteristics of domain architecture, the twenty-one JmjC domain-containing proteins were first divided into two groups (Groups I and II); each group was then further divided into several clades: Group I was divided into Clades I and II; Group II was divided into Clades III, IV, and V. One remarkable difference between Groups I and II is the JmjN domain: Eight out of nine JmjC domain-containing proteins belonging to the first group contain a JmjN domain N-terminal to the JmjC domain, whereas none of the twelve proteins of Group II has it (Fig. 1). Although the role of this domain is not clear yet, its deletion from JMJD2A results in a loss of enzyme activity (Chen et al., 2006), suggesting that the JmjN domain may be necessary for the function of some Jmj proteins.

Three Jmj proteins encoded by *AtJmj3, ELF6,* and *REF6* formed Clade I of Group I *Arabidopsis* JmjC domain-containing proteins. ELF6 and REF6, as previously reported (Noh et al., 2004), were identical in domain structure and had JmjN and JmjC domains as well as four copies of C2H2-type zinc-finger (ZnF) motif that might serve as a DNA-binding domain. However, unlike ELF6 and REF6, AtJmj3 did not contain a C2H2-type ZnF motif. In addition, Atjmj3 is expected to be smaller than either ELF6 or REF6.

The other six Jmj proteins in Group I, AtJmj4 to AtJmj9, were clustered in Clade II. Clade II proteins showed a domain architecture that was distinct from the proteins of the other clades. They were further sub-grouped based on their domain composition and architecture. AtJmj 4, 5, 6, and 8 were identical in domain architecture, having JmjN, JmjC, a single C5HC2 ZnF, and FYRN/FYRC domains at their C-termini. The C5HC2 ZnF is found in JmjC domain-containing proteins and may be involved in DNA binding (Clissold and Ponting, 2001). FYRN/FYRC domains are usually found together in Trithorax and its homologs, which are H3K4 methyltransferases (Finn et al., 2006). In contrast, AtJmj9 has JmjN, JmjC, and C5HC2 ZnF domains but no FYRN/FYRC domain. AtJmj7 was the only protein in Group I (Clade I and Clade II) that does not contain a JmjN domain; it contains only a JmjC domain. Notably, although a single C5HC2 ZnF was found, the C-terminus of AtJmj7 also has a plant homeodomain (PHD) finger, which is believed to be a chromatin-binding domain (Musco and Peterson, 2008).

Whereas most members of Group I contained both of JmjN and JmjC domains, none of the twelve members of Group II (Clades III, IV, and V) contain a JmjN domain. AtJmj12, AtJmj14,

Table 2. Oligonucleotides used for RT-PCR analysis

Gene	Name	Sequence
AtJmj3	JMJ3-exon1/2-F′	5′-GCAAATGGAACTTGAATAAAGTTTC-3′
	JMJ3-exon1/2-R′	5′-CTCACCACAATTAAAACCGTGGCT-3′
AtJmj4	JMJ4-F	5′-GCAGAGTCTGTGGCTATGG-3′
	JMJ4-R	5′-CCAGGGTAAAATCTGGCCC-3′
AtJmj5	JMJ5-exon1/2-F′	5′-GGCGTTGTCATCGAAAGAACAAGG-3′
	JMJ5-exon1/2-R′	5′-AGCGTATCTTCAAACTCCTCTGAT
AtJmj6	JMJ6-F	5′-GCCATCTGTTCCTCCTGG-3′
	JMJ6-R	5′-CTTTCAGTGGGCACGGCGG-3′
AtJmj7	JMJ7-F	5′-GATGAGTATTGTGGTAGCCC-3′
	JMJ7-R	5′-CCCTTCGTTATTGCAGCAG-3′
AtJmj8	JMJ8-F	5′-CGAGAAGATACGTCCACTAG-3′
	JMJ8-R	5′-TACAGAGCCAGGAAGCCG-3′
AtJmj9	JMJ9-F	5′-GACACAATTTCTGCTCCG-3′
	JMJ9-R	5′-ATCTTTCGGTTCTCGGTCTG-3′
AtJmj10	JMJ10-F	5′-GTGCCAAAAGAAGAAGGACG-3′
	JMJ10-R	5′-TTCCCATGATTCAGCAGTCCG-3′
AtJmj11	JMJ11-F	5′-TCCAGCCGGATCAGGATCG-3′
	JMJ11-R	5′-CTCTCTGTCAGTTGTCCCG-3′

AtJmj15, AtJmj16, AtJmj17, and AtJmj18 clustered in CladeIII. Among them, AtJmj12, AtJmj14, AtJmj17, and AtJmj18 contain a RING-finger domain, which is implicated in a protein-protein interaction (Kosarev et al., 2002). Three proteins, AtJmj10, AtJjmj11, and AtJmj13, were grouped in Clade IV. Interestingly, both AtJmj10 and AtJmj11 have an F-box domain at their N-termini. Because F-box domain-containing proteins are known to mediate protein ubiquitylation, the histone demethylation by these Jmj proteins might accompany the ubiquitylation of the same histones or other proteins functionally connected to them. The last three *Arabidopsis* Jmj proteins identified, AtJmj19, AtJmj20, and AtJmj21, formed Clade V, which contained no recognizable domains aside from JmjC domains. The predicted lengths of these proteins are also shorter than those of the AtJmj proteins of the other clades.

mRNA expression patterns of *AtJmj* genes in various tissues

In order to gain insight into the roles of *Arabidopsis* JmjC domain-containing proteins, we examined the expression of the nine *AtJmj* genes in various vegetative and reproductive tissues, such as seedlings, rosette leaves, shoot apices with young leaves, roots, and flowers by RT-PCR (Fig. 2). Most of the nine *AtJmj* mRNAs (except for *AtJmj5* mRNA) were expressed in all tissues examined. Expression of *AtJmj5* mRNA was not detected in the root or in the shoot apices with young leaves. Notably, all *AtJmj* genes showed relatively higher mRNA expression in flowers compared to other tissues. Although AtJmj10 and AtJmj11 are closely related each other in our phylogenetic analysis, their mRNA expression patterns were distinct from each other. The expression level of *AtJmj10* mRNA was high in seedlings, roots and flowers; whereas *AtJmj11* mRNA was rather weakly expressed in seedlings and roots compared to in flowers.

Histochemical analysis of the expression of *AtJmj* genes

We next investigated the temporal and spatial expression patterns of *AtJmj3* to *AtJmj11* using *GUS* reporter fusions (Figs. 3-11).

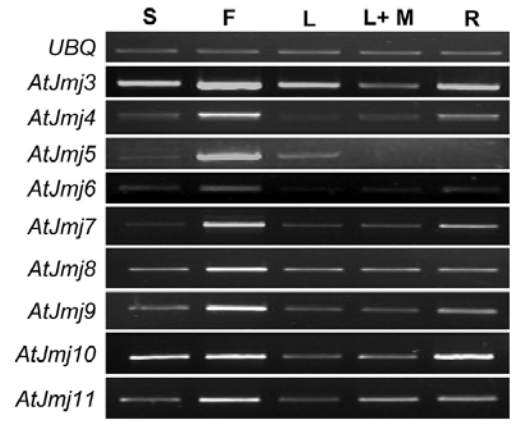

Fig. 2. RT-PCR analyses of mRNA expression of the nine *AtJmj* genes in various tissues. S, seedling; F, flower; L, leaf; L + M, young leaf with shoot apical meristematic region; R, root. *Ubiquitin 10* (*UBQ*) was used as an expression control.

Clade I: *AtJmj3, ELF6,* and *REF6*

We previously reported the GUS expression patterns of *ELF6* and *REF6* (Noh et al., 2004). Although they are closely related genes, their GUS expression patterns were distinct from each other. In case of $REF6_{pro}$*::REF6:GUS* fusion, GUS staining was observed in the shoot apex, root tips, cotyledons, leaves, root axis, and vascular tissues; whereas $ELF6_{pro}$*::ELF6:GUS* was expressed at low levels in cotyledons and leaves. The expression pattern of $AtJmj3_{pro}$*::GUS* was similar to that of $REF6_{pro}$*::REF6:GUS*; strong GUS staining was detected in the shoot apex, trichomes, lateral roots, and root tips (Fig. 3). Notably, the intensity of GUS staining was higher in the lateral roots than in the primary root (Fig. 3F). In floral organs, $AtJmj3_{pro}$*::GUS* was strongly expressed in mature pollen grains and stigmatic papillae (Figs. 3K and 3L) but weakly expressed in the egg cell region (Fig. 3M).

Clade II: *AtJmj 4, 5, 6, 7, 8,* and *9*

GUS expression patterns driven by the promoters of *AtJmj* genes belonging to Clade II (Figs. 4-9) were largely divided into two types. GUS staining of plants carrying either $AtJmj5_{pro}$*::GUS* or $AtJmj7_{pro}$*::GUS* was weak and only detected in a limited range of tissues. Compared with the GUS activity of $AtJmj5_{pro}$*::GUS* and $AtJmj7_{pro}$*::GUS*, stronger GUS expression was observed in more various tissues of the transgenic plants carrying *promoter::GUS* fusions for *AtJmj4*, *AtJmj6* to *9*.

The expression of $AtJmj5_{pro}$*::GUS* was weak and localized in the tips of cotyledons and the hypocotyls of seedlings as well as in mature pollen grains of stamen (Fig. 5). This GUS expression pattern was consistent with the mRNA expression pattern studied by RT-PCR (Fig. 2). GUS staining of transgenic plants harboring $AtJmj7_{pro}$*::GUS* was also weak and tissue-specific (Fig. 7). In young seedlings, weak GUS expression was observed in the tips of cotyledons (Fig. 7B). In older plants, GUS staining was detected in the shoot apex and vascular tissues of cotyledons and leaves but not in any part of the root (Figs. 7C, 7D, and 7G-7J). In flowers, weak GUS staining was observed in pollen grains and the funiculus of ovule (Figs. 7K and 7L).

$AtJmj4_{pro}$*::GUS* was expressed in various tissues throughout development, including cotyledons, leaves, roots and flowers

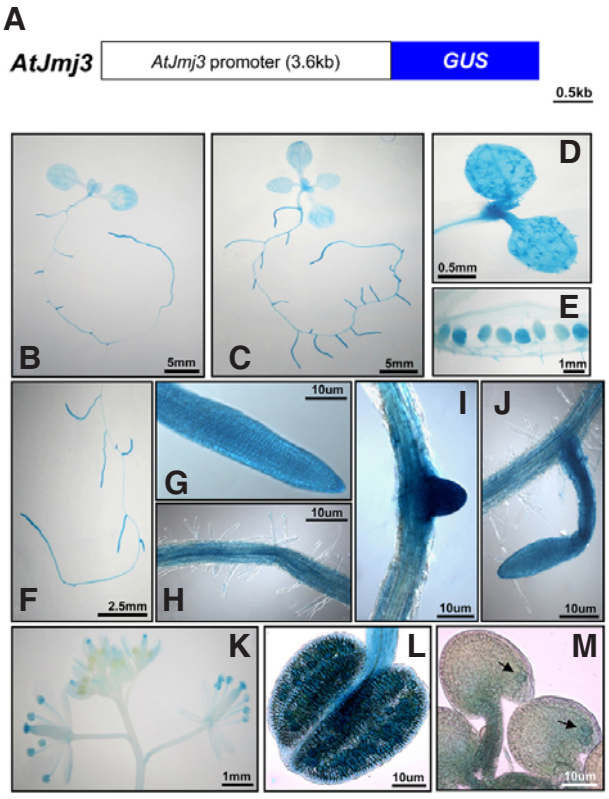

Fig. 3. Expression pattern of *AtJmj3*$_{pro}$*::GUS*. (A) Schematic of the *AtJmj3*$_{pro}$*::GUS* fusion construct. (B-M) Histochemical GUS analysis of transgenic *Arabidopsis* containing the *AtJmj3*$_{pro}$*::GUS*. (B) Seven-d-old seedling. (C) Fourteen-d-old seedling. (D) Trichomes and shoot apex of seven-d-old seedling. (E) Silique. (F) Root of ten-d-old seedling. (G) Primary root tip. (H) Root hairs. (I, J) Developing lateral roots. (K) Flowers. (L) Stamen. (M) Ovules. Arrows indicate regions containing the egg cells. All plants were grown in long days (LD; 16 h day/8 h night).

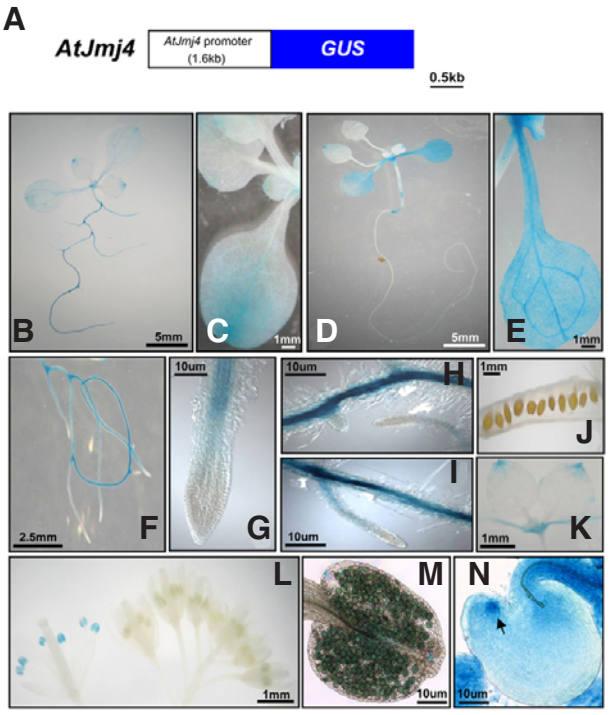

Fig. 4. Expression pattern of *AtJmj4*$_{pro}$*::GUS*. (A) Schematic of the *AtJm4*$_{pro}$*::GUS* fusion construct. (B-N) Histochemical GUS analysis of transgenic *Arabidopsis* containing the *AtJmj4*$_{pro}$*::GUS*. (B, C) LD-grown seven-d-old seedling. (D, E) SD-grown ten-d-old seedling. (F) Root of LD-grown ten-d-old seedling. (G) Primary root tip of LD-grown seedling. (H, I) Developing lateral roots of LD-grown seedling. (J) Silique. (K) Shoot apex of LD-grown seven-d-old seedling. (L) Flowers. (M) Stamen. (N) Ovule. Arrow indicates a region containing the egg cell.

(Fig. 4). Interestingly, the GUS staining pattern of *AtJmj4*$_{pro}$*::GUS* was affected by day length. In long days (LD; 16 h day/8 h night), the GUS staining was detected in aerial tissues and more strongly in roots (Figs. 4B and 4C); whereas in short days (SD; 8 h day/ 16 h night), GUS staining was not detectable in the roots, but was detectable in aerial parts, like cotyledons (Figs. 4D and 4E). These results suggest that the spatial expression of *AtJmj4* is likely to be regulated by photoperiod, which might reflect the biological function of this gene. *AtJmj4*$_{pro}$*::GUS* expression was mainly detected in the root regions containing non-dividing cells, but not in the root regions where cells actively divide such as root tips or newly emerging lateral roots (Figs. 4F-4I). *AtJmj4*$_{pro}$*::GUS* was also expressed in reproductive tissues such as mature pollen grains and the egg cell (Figs. 4L-4N).

In young seedlings, *AtJmj6*$_{pro}$*::GUS* was expressed in the tips of cotyledons, hypocotyls, the shoot apex, and the root (Fig. 6B). In older seedlings, GUS staining was stronger and more widely distributed in cotyledons and leaves including trichomes (Figs. 6C and 6J). The expression of *AtJmj6*$_{pro}$*::GUS* in roots was localized in regions where lateral roots began to emerge, but not in the elongating lateral roots or primary root tips (Figs. 6D-6F). During the reproductive stage, *AtJmj6*$_{pro}$*::GUS* was highly expressed in mature pollen grains and ovules (Figs. 6H and 6I), and was expressed at low level in seeds (Fig. 6K).

Expression of *AtJmj8*$_{pro}$*::GUS* was detected in most vegetative tissues except root tips (Fig. 8). Like *AtJmj6*$_{pro}$*::GUS*, *AtJmj8*$_{pro}$*::GUS* was highly expressed in root regions where lateral roots emerged, but not in the elongating lateral roots or primary root tips (Figs. 8C-8E). In flowers, strong GUS staining was observed in pollen grains, stigmas, and ovules (Figs. 8H-8J). In ovules, *AtJmj8*$_{pro}$*::GUS* expression was localized in the regions containing the egg cell and the antipodal cells (Fig. 8J). Its expression was strong in the vascular tissues of cotyledons and leaves and also in trichomes (Figs. 8F and 8G).

Like *AtJmj4*$_{pro}$*::GUS, AtJmj6*$_{pro}$*::GUS, and AtJmj8*$_{pro}$*::GUS, AtJmj9*$_{pro}$*::GUS* was also expressed in various tissues, but showed a distinct expression pattern (Fig. 9). In young seedlings, GUS staining was observed in cotyledons, the shoot apex, and roots (Fig. 9B). GUS staining was stronger in roots than in aerial tissues, and no GUS staining was observed in root tips or lateral roots (Figs. 9G-9J). In older plants, *AtJmj9*$_{pro}$*::GUS* expression was detected in leaves, especially in trichomes (Figs. 9C-9E). In flowers, its expression was detected in most of the floral organs, such as stigmas, pollen grains, and filaments, but not in ovules (Figs. 9K-9M).

Clade IV: *AtJmj 10* and *11*

Expression patterns of *AtJmj10*$_{pro}$*::AtJmj10:GUS* and *AtJmj11*$_{pro}$*::AtJmj11:GUS* were similar to each other in vegetative tissues (Figs. 10B-10I and 11B-11I), suggesting that structurally related

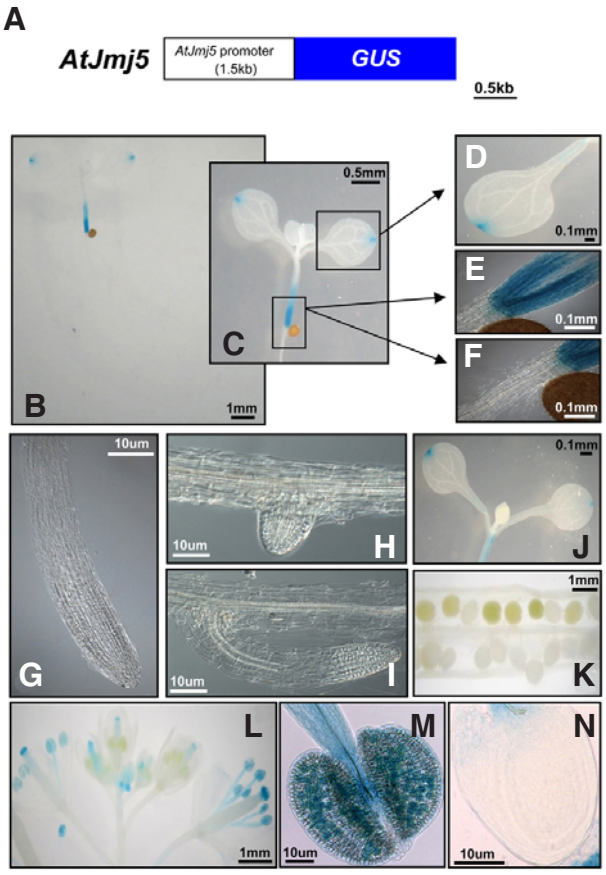

Fig. 5. Expression pattern of *AtJmj5*$_{pro}$*::GUS*. (A) Schematic of the *AtJmj5*$_{pro}$*::GUS* fusion construct. (B-N) Histochemical GUS analysis of transgenic *Arabidopsis* containing the *AtJmj5*$_{pro}$*::GUS*. (B-F) Seven-d-old seedling. (D) Cotyledon. (E, F) Hypocotyl and root transition zone. (G) Primary root tip. (H, I) Developing lateral roots. (J) Shoot apex of seven-d-old seedling. (K) Silique. (L) Flowers. (M) Stamen. (N) Ovule. All plants were grown in LD.

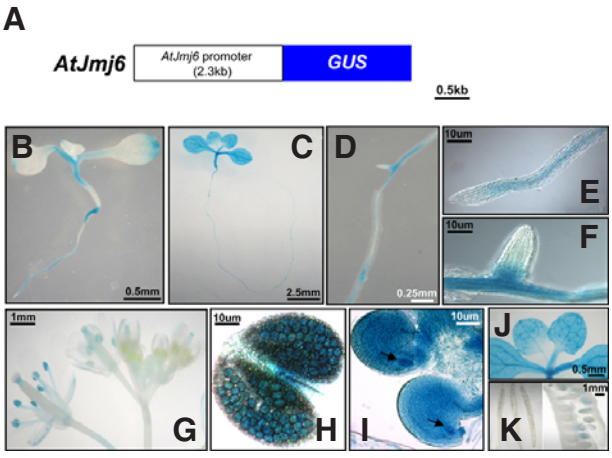

Fig. 6. Expression pattern of *AtJmj6*$_{pro}$*::GUS*. (A) Schematic of the *AtJmj6*$_{pro}$*::GUS* fusion construct. (B-K) Histochemical GUS analysis of transgenic *Arabidopsis* containing the *AtJmj6*$_{pro}$*::GUS*. (B) Seven-d-old seedling. (C) Fourteen-d-old seedling. (D) Root of ten-d-old seedling. (E) Primary root tip. (F) Developing lateral root. (G) Flowers. (H) Stamen. (I) Ovules. Arrows indicate regions containing the egg cells. (J) Shoot apex of seven-d-old seedling. (K) Siliques. All plants were grown in LD.

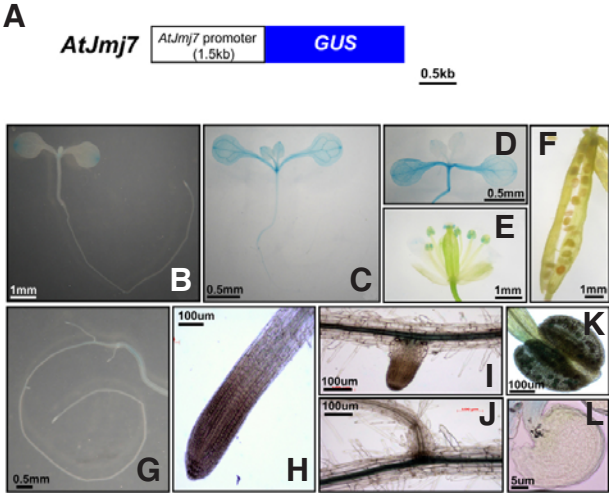

Fig. 7. Expression pattern of *AtJmj7*$_{pro}$*::GUS*. (A) Schematic of the *AtJmj7*$_{pro}$*::GUS* fusion construct. (B-L) Histochemical GUS analysis of transgenic *Arabidopsis* containing the *AtJmj7*$_{pro}$*::GUS*. (B) Seven-d-old seedling. (C) Ten-d-old seedling. (D) Shoot apex of seven-d-old seedling. (E) Flowers. (F) Silique. (G) Root of ten-d-old seedling. (H) Primary root tip. (I and J) Developing lateral roots. (K) Stamen. (L) Ovule. All plants were grown in LD.

these two genes might perform similar functions in these tissues. Expression of both *AtJmj10*$_{pro}$*::AtJmj10:GUS* and *AtJmj11*$_{pro}$*::AtJmj11:GUS* was detected in the shoot apex, cotyledons, leaves, and roots. Unlike the *GUS* expression driven by the promoters of *AtJmj* genes in Clade II, the expression of *AtJmj10*$_{pro}$*::AtJmj10:GUS* and *AtJmj11*$_{pro}$*::AtJmj11:GUS* was high in root tips and lateral roots (Figs. 10F-10H and 11F-11H). Although these two genes showed similar expression patterns in vegetative tissues, their expression patterns in floral organs were quite distinct from each other. *AtJmj10*$_{pro}$*::AtJmj10:GUS* was expressed in many floral organs such as sepals, petals, filaments, stigmas, pollen grains, and also weakly in ovules (Figs. 10K-10M). However, *AtJmj11*$_{pro}$*::AtJmj11:GUS* expression was detected only weakly in stigmas but not in the other floral organs (Figs. 11K-11M). These results suggest that *AtJmj10* and *AtJmj11* might play divergent roles during reproductive development.

DISCUSSION

The genes encoding JmjC domain-containing proteins represent a large gene family in numerous organisms: there are thirty in human, thirty in mouse, thirteen in *Drosophila melanogaster*, thirteen in *Caenorhabditis elegans*, seven in fission yeast, and five in budding yeast (Klose et al., 2006). In plants, bioinformatic analysis has identified twenty-one *Arabidopsis* genes and twenty rice genes that encode JmjC domain-containing proteins (Lu et al., 2008 and this study). The large numbers of these genes suggest that they may play key roles in diverse biological processes. In the present study, as an initial step in uncovering the roles of JmjC domain-containing proteins in *Arabidopsis*, we identified genes encoding putative JmjC domain-containing proteins from the *Arabidopsis* genome

Table 3. Spatial expression patterns of *AtJmj* genes in various tissues

Tissues	Clade I	Clade II					Clade IV		
	AtJmj3	*AtJmj4*	*AtJmj5*	*AtJmj6*	*AtJmj7*	*AtJmj8*	*AtJmj9*	*AtJmj10*	*AtJmj11*
Seedling									
cotyledon	+	+	-	++	+	++	+++	+++	+++
leaf	+	-	-	+	+	++	++	+++	++
hypocotyl	++	-	++	++	+	++	-	-	+
hypocotyl/root transition	+	+	++	++	+	++	+	++	++
Shoot apex	+++	++	-	++	++	++	+++	+++	+++
Root									
primary	+	++	+	+	+	++	+++	+++	+++
lateral	+++	-	-	-	-	-	-	+++	+++
tip	+++	-	-	-	-	-	+++	+++	++
Rosette leaf	+	+	-	+	+	++	++	++	++
Flower						-			
stigma	++	-	++	++	-	++	++	++	+
ovule	+	++	-	+++	-	-	-	+	-
stamen									
pollen	+++	+	++	+++	+	+++	++	+++	-
filament	++	-	++	++	-	-	++	+	-
petal	+	-	-	+	-	+++	+++	+	-
sepal	+	-	-	++	-	++	+++	++	-

The + and - indicate intensity of GUS staining: -, negative; +, weak; ++, intermediate; +++, strong.

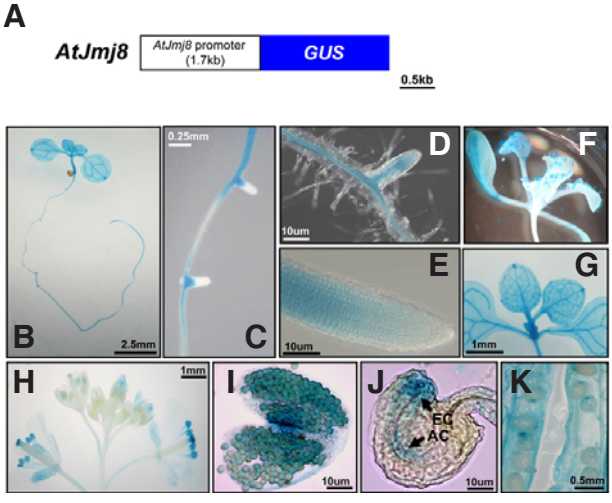

Fig. 8. Expression pattern of *AtJmj8*$_{pro}$*::GUS*. (A) Schematic of the *AtJmj8*$_{pro}$*::GUS* fusion construct. (B-K) Histochemical GUS analysis of transgenic *Arabidopsis* containing the *AtJmj8*$_{pro}$*::GUS*. (B) Ten-d-old seedling. (C, D) Developing lateral roots. (E) Primary root tip. (F) Expression in trichomes. (G) Shoot apex of ten-d-old seedling. (H) Flowers. (I) Stamen. (J) Ovule. Arrows indicate regions containing the egg cell (EC) and the antipodal cells (AC). (K) Siliques. All plants were grown in LD.

and analyzed both their phylogenetic relationships and their spatial and temporal expression patterns.

Based on sequence similarity and the features of domain architecture of *Arabidopsis* JmjC domain-containing proteins, we grouped them into five clades. Recently, Lu et al. (2008) clustered the JmjC domain-containing proteins of *Arabidopsis* and rice into eight groups. Because *Arabidopsis* lacks three of these groups that exist in rice-namely, members of the KDM6/JMJD3, KDM2/JHDM1, and PHF groups-the classification of Lu et al. (2008) actually agrees well with ours.

Up to now, no biochemical analysis of *Arabidopsis* JmjC domain-containing proteins has been reported. However, phylogenetic analyses with human JmjC domain-containing proteins whose biochemical functions are known might provide hints of the possible biochemical activities of *Arabidopsis* JmjC domain-containing proteins of each clade. Our phylogenetic analysis of *Arabidopsis* and human JmjC domain-containing proteins (data not shown) revealed that AtJmj proteins belonging to Clade II are grouped with JARID1 proteins that demethylate mono-, di- and trimethylated H3K4 (Xiang et al., 2007). Clade III AtJmj proteins are similar to JMJD1 proteins, which are known to demethylate mono- and dimethylated H3K9 (Yamane et al., 2006). Histone arginine demethylase JMJD6 (Chang et al., 2007) was grouped with the Clade IV AtJmj proteins. The members of Clades I and V were not clearly grouped with any of the human JmjC domain-containing proteins. In addition, none of the *Arabidopsis* JmjC domain-containing proteins were clustered with either UTY (which demethylate di- and trimethylated H3K27 (Agger et al., 2007)) or JMJD2 proteins (which demethylate di- and trimethylated H3K9 or H3K36 (Whetstine et al., 2006)). Thus, phylogenetic analyses suggest that *Arabidopsis* has both evolutionarily conserved types of JmjC domain-containing proteins and plant-specific types.

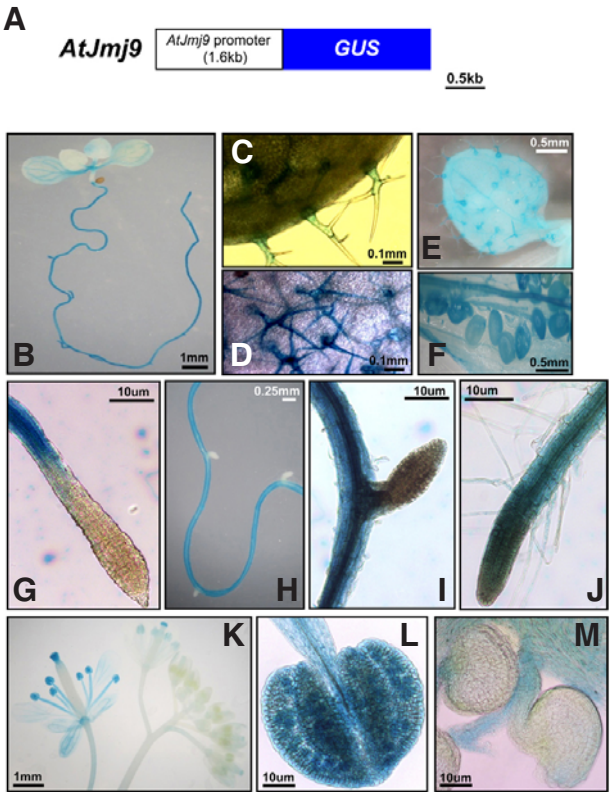

Fig. 9. Expression pattern of *AtJmj9*$_{pro}$*::GUS*. (A) Schematic of the *AtJmj9*$_{pro}$*::GUS* fusion construct. (B-M) Histochemical GUS analysis of transgenic *Arabidopsis* containing the *AtJmj9*$_{pro}$*::GUS*. (B) Seven-d-old seedling. (C-E) Expression in trichomes. (F) Silique. (G) Primary root tip. (H and I) Developing lateral roots. (J) Primary root tip and root hairs. (K) Flowers. (L) Stamen. (M) Ovules. All plants were grown in LD.

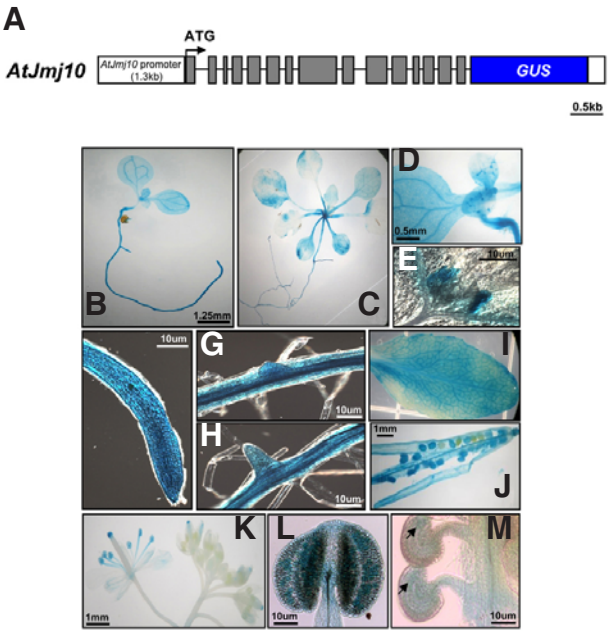

Fig. 10. Expression pattern of *AtJmj10*$_{pro}$*::AtJmj10:GUS*. (A) Schematic of the *AtJmj10*$_{pro}$*::AtJmj10:GUS* fusion construct. Gray boxes indicate exons, whereas lines are introns. (B-M) Histochemical GUS analysis of transgenic *Arabidopsis* containing the *AtJmj10*$_{pro}$*::AtJmj10:GUS*. (B) Seven-d-old seedling. (C) Seventeen-d-old plant. (D, E) Shoot apex of seven-d-old seedling. (F) Primary root tip. (G, H) Developing lateral roots. (I) Leaf from one-month-old plant. (J) Silique. (K) Flowers. (L) Stamen. (M) Ovules. Arrows indicate regions containing the egg cells. All plants were grown in LD.

RT-PCR analyses indicate that all *AtJmj* genes studied in this report are actively expressed (Fig. 2). In addition, their mRNA expression patterns varied among the different plant organs. In particular, the mRNA expression levels in flowers were generally higher than in other tissues. This mRNA expression analysis agrees well with the results of the histochemical GUS analysis (Figs. 3-11), and a summary for the spatial expression pattern analyses is presented in Table 3. Most *AtJmj::GUS* fusion constructs showed expression in either stigmas or pollen grains. It is not known whether these *AtJmj* genes function in floral or reproductive development, however, these expression data may suggest possible roles of histone demethylases in such processes.

There are three genes in Clade I: *ELF6*, *REF6*, and *AtJmj3*. Despite their sequence similarities, *ELF6* and *REF6* have quite distinct expression patterns and biological roles (Noh et al., 2004). The expression pattern of *AtJmj3* was similar to that of *REF6* (Fig. 3). Thus, it is possible that *AtJmj3* plays a role redundant to *REF6* rather than to *ELF6*. Currently, we are testing this possibility.

The expression patterns of members of Clade II can be roughly divided into two types. *AtJmj4*, *6*, *8*, and *9* tend to be expressed in various tissues. Interestingly, the expression of these genes was not detected in the tips of primary and lateral roots, whereas their expression was detected in the basal parts of the root (Figs. 4, 6, 8, and 9). It is known that cells in primary and lateral root tips are actively dividing while cells in the basal parts of primary and lateral roots are not; instead they are growing through cell expansion (Malamy and Bendey, 1997). Thus, it is likely that *AtJmj4*, *6*, *8*, and *9* might be involved in repressing cell division activities in the basal parts of the root. In contrast, the expression patterns of *AtJmj5* and *7* were tissue-specific (Figs. 5 and 7), suggesting that their function(s) would be more specific relative to other members. For example, *AtJmj5* was expressed at low levels in vegetative tissues; however, a higher expression level was observed in flowers by RT-PCR (Fig. 2). Histochemical GUS analysis confirmed the RT-PCR data and showed that the expression in flowers occurs mainly in pollen grains (Fig. 5). Interestingly, *AtJmj5* was reported to be involved in gametophyte development (as *MEE27*; Pagnussat et al., 2005). Thus, it seems that the specific expression pattern of *AtJmj5* is related to its mutant phenotype.

Two members of Clade IV, AtJmj10 and AtJmj11, are similar in both their JmjC-domain sequences and domain architectures (Fig. 1). The expression pattern of these two genes was also similar in vegetative tissues (Figs. 10 and 11). They are expressed in most vegetative tissues, suggesting that they might have diverse roles during vegetative development. However, they exhibited distinct expression patterns during reproductive development. In the case of *AtJmj11*, no expression was detected in pollen grains, stamens, or ovules. Like the case of *ELF6* and *REF6*, it is possible that *AtJmj10* and *AtJmj11* have divergent roles, especially in the reproductive tissues.

Our studies on the phylogenetic relationship of the twenty-one *Arabidopsis* JmjC domain-containing proteins and the spatiotemporal expression patterns of nine of them show that there

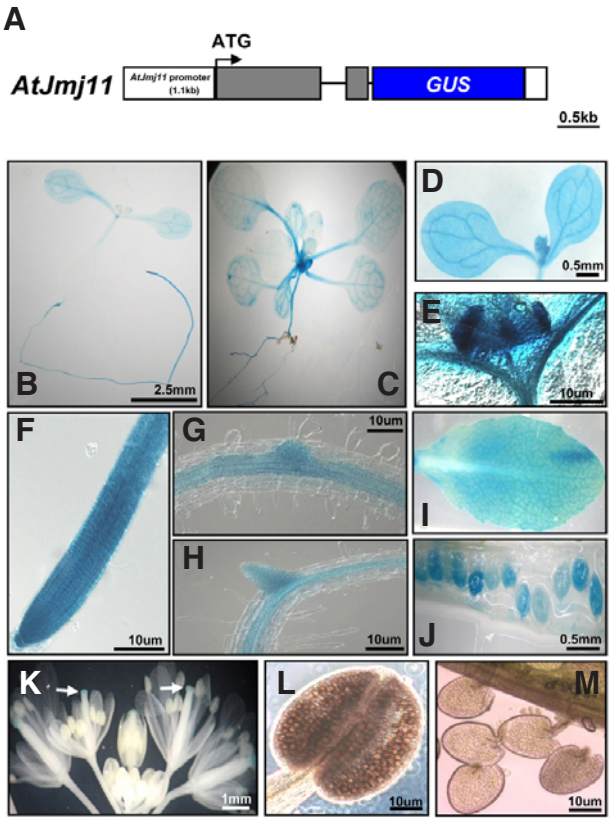

Fig. 11. Expression pattern of *AtJmj11*$_{pro}$*::AtJmj11:GUS*. (A) Schematic of the *AtJmj11*$_{pro}$*::AtJmj11:GUS* fusion construct. Gray boxes indicate exon, and lines are introns. (B-M) Histochemical GUS analysis of transgenic *Arabidopsis* containing the *AtJmj11*$_{pro}$*::AtJmj11:GUS*. (B) Seven-d-old seedling. (C) Seventeen-d-old plant. (D, E) Shoot apex of seven-d-old seedling. (F) Primary root tip. (G, H) Developing lateral roots. (I) Leaf from one-month-old plant. (J) Silique. (K) Flowers. White arrows indicate stigmas (L) Stamen. (M) Ovules. All plants were grown in LD.

is some degree of correlation between the phylogenetic relationship and the expression pattern. However, despite similarities in sequences and domain architecture within clades, some members in the same clade exhibited diverse and distinct expression patterns, as shown in the case of *ELF6* and *REF6* (Noh et al., 2004), *AtJmj5* and *AtJmj8*, and *AtJmj10* and *AtJmj11*. Thus, taken together, *AtJmj* genes within the same phylogenetic groups might share expression domains and biological functions. However, some of the genes within the same group can have unique roles during *Arabidopsis* development and responses to internal and external stimuli. Combined with present study, future genetic characterization and biochemical studies on their protein products will address the detailed roles of *AtJmj* genes.

ACKNOWLEDGMENTS

This work was supported by the GRL Program of the Ministry of Education, Science and Technology/Korea Foundation for International Cooperation of Science and Technology, by the Plant Diversity Research Center, and by the BioGreen21 Program of the RDA. B.N. was supported by a grant from the Ministry of Education, Science and Technology/Korea Science and Engineering Foundation to the Environmental Biotechnology National Core Research Center (R15-2003-012-01001-0) and by grants from the Korea Research Foundation (KRF-2007-313-C00703 and KRF-2006-312-C00672). E.-H.H. was supported by the Brain Korea 21 Program.

REFERENCES

Agger, K., Cloos, P.A., Christensen, J., Pasini, D., Rose, S., Rappsilber, J., Issaeva, I., Canaani, E., Salcini, A.E., and Helin, K. (2007). UTX and JMJD3 are histone H3K27 demethylases involved in HOX gene regulation and development. Nature *449*, 731-734.

Byvoet, P. (1972). *In vivo* turnover and distribution of radio-N-methyl in arginine-rich histones from rat tissues. Arch. Biochem. Biophys. *152*, 887-888.

Chang, B., Chen, Y., and Bruick, R.K. (2007). JMJD6 is a histone arginine demethylase, Science *318*, 444-447.

Chen, Z., Zang, J., Whetstine, J., Hong, X., Davrazou, F., Kutateladze, T.G., Simpson, M., Mao, Q., Pan, C.H., Dai, S., et al. (2006). Structural insights into histone demethylation by JMJD2 family members. Cell *125*, 691-702.

Clissold, P.M., and Ponting, C.P. (2001). JmjC: cupin metalloenzyme-like domains in jumonji, hairless and phospholipase A2beta. Trends Biochem. Sci. *26*, 7-9.

Cloos, P.A.C., Christensen, J., Agger, K., Maiolica, A., Rappsilber, J., Antal, T., Hansen, K.H., and Helin, K. (2006). The putative oncogene GASC1 demethylates tri- and dimethylated lysine 9 on histone H3. Nature *442*, 307-311.

Clough, S.J., and Bent, A.F. (1998). Floral dip: a simplified method for Agrobacterium-mediated transformation of *Arabidopsis thaliana*. Plant J. *16*, 735-743.

Cuthbert, G.L., Daujat, S., Snowden, A.W., Erdjument-Bromage, H., Hagiwara, T., Yamada, M., Schneider, R., Gregory, P.D., Tempst, P., Bannister, A.J., et al. (2004). Histone deimination antagonizes arginine methylation. Cell *118*, 545-553.

Duerre, J.A., and Lee, C.T. (1974). *In vivo* methylation and turnover of rat brain histones. J. Neurochem. *23*, 541-547.

Finn, R.D., Mistry, J., Schuster-Böckler, B., Griffiths-Jones, S., Hollich, V., Lassmann, T., Moxon, S., Marshall, M., Khanna, A., Durbin, R., et al. (2006). Pfam: clans, web tools and services. Nucleic Acids Res. *34*, D247-251.

Jefferson, R.A., Kavanagh, T.A., and Bevan, M.W. (1987). GUS fusions: beta-glucuronidase as a sensitive and versatile gene fusion marker in higher plants. EMBO J. *6*, 3901-3907.

Klose, R.J., Kallin, E.M., and Zhang, Y. (2006). JmjC-domain-containing proteins and histone demethylation. Nat. Rev. Genet. *7*, 715-727.

Kosarev, P., Mayer, K.F., and Hardtke, C.S. (2002). Evaluation and classification of RING-finger domains encoded by the Arabidopsis genome. Genome Biol. 3, RESEARCH0016.

Kouzarides, T. (2007). Chromatin modifications and their function. Cell *128*, 693-705.

Kwon, S.H., and Workman, J.L. (2008). The heterochromatin protein 1 (HP1) family: put away a bias toward HP1. Mol. Cells *26*, 217-227.

Lu, F., Li, G., Cui, X., Liu, C., Wang, X.J., and Cao, X. (2008). Comparative analysis of JmjC domain-containing proteins reveals the potential histone demethylases in *Arabidopsis* and rice. J. Int. Plant Biol. *50*, 886-896.

Malamy, J., and Benfey, P. (1997). Organization and cell differentiation. Development *124*, 33-44.

Martin, C., and Zhang, Y. (2005). The diverse functions of histone lysine methylation. Nat. Rev. Mol. Cell. Biol. *6*, 838-849.

Musco, G., and Peterson, P. (2008). PHD finger of autoimmune regulator: An epigenetic link between the histone modifications and tissue-specific antigen expression in thymus. Epigenetics *3*, 310-314.

Noh, Y.S., and Amasino, R.M. (2003). *PIE1*, an *ISWI* family gene, is required for *FLC* activation and floral repression in Arabidopsis. Plant Cell *15*, 1671-1682.

Noh, B., Lee, S.H., Kim, H.J., Yi, G., Shin, E.A., Lee, M., Jung, K.J., Doyle, M.R., Amasino, R.M., and Noh, Y.S. (2004). Divergent roles of a pair of homologous Jumonji/zinc-finger-class transcription factor proteins in the regulation of Arabidopsis flowering

time. Plant Cell *16*, 2601-2613.
Pagnussat, G.C., Yu, H.J., Ngo, Q.A., Rajani, S., Mayalagu, S., Johnson, C.S., Capron, A., Xie, L.F., Ye, D., and Sundaresan, V. (2005). Genetic and molecular identification of genes required for female gametophyte development and function in Arabidopsis. Development *132*, 603-614.
Saze, H., Shiraishi, A., Miura, A., and Kakutani, T. (2008). Control of genic DNA methylation by a jmjC domain-containing protein in *Arabidopsis thaliana*. Science *319*, 462-465.
Shi, Y., Lan, F., Matson, C., Mulligan, P., Whetstine, J.R., Cole, P.A., Casero, R.A., and Shi, Y. (2004). Histone demethylation mediated by the nuclear amine oxidase homolog LSD1. Cell *119*, 941–953.
Thompson, J.D., Higgins, D.G., and Gibson, T.J. (1994). CLUSTAL W: improving the sensitivity of progressive multiple sequence alignment through sequence weighting, position-specific gap penalties and weight matrix choice. Nucleic Acids Res. *22*, 4673-4680.
Tsukada, Y., Fang, J., Erdjument-Bromage, H., Warren, M.E., Borchers, C.H., Tempst, P., and Zhang, Y. (2006). Histone demethylation by a family of JmjC domain-containing proteins. Nature *439*, 811-816.
Whetstine, J.R., Nottke, A., Lan, F., Huarte, M., Smolikov, S., Chen, Z., Spooner, E., Li, E., Zhang, G., Colaiacovo, M., et al. (2006). Reversal of histone lysine trimethylation by the JMJD2 family of histone demethylases. Cell *125*, 467-481.
Xiang, Y., Zhu, Z., Han, G., Ye, X., Xu, B., Peng, Z., Ma, Y., Yu, Y., Lin, H., Chen, A.P., et al. (2007). JARID1B is a histone H3 lysine 4 demethylase up-regulated in prostate cancer. Proc. Natl. Acad. Sci. USA *103*, 19226-19231.
Yamane, K., Toumazou, C., Tsukada, Y., Erdjument-Bromage, H., Tempst, P., Wong, J., and Zhang, Y. (2006). JHDM2A, a JmjC-containing H3K9 demethylase, facilitates transcription activation by androgen receptor. Cell *125*, 483-495.
Zhou, X., and Ma, H. (2008). Evolutionary history of histone demethylase families: distinct evolutionary patterns suggest functional divergence. BMC Evol. Biol. *8*, 294.